NÖHÜ Müh. Bilim. Derg. / NOHU J. Eng. Sci., Erken Görünüm / In Press
Niğde Ömer Halisdemir Üniversitesi Mühendislik Bilimleri Dergisi
Niğde Ömer Halisdemir University Journal of Engineering Sciences
Araştırma makalesi / Research article
www.dergipark.org.tr/tr/pub/ngumuh / www.dergipark.org.tr/en/pub/ngumuh

# Modeling approach for estimation of ultimate load capacity of concrete-filled steel tube composite stub columns based on relevance vector machine

## Beton-dolgulu çelik tüplü kompozit kısa kolonların nihai yük taşıma kapasitesinin ilgililik vektör makinesine dayalı tahmini için modelleme yaklaşımı

**Çiğdem Avcı Karataş**[1,*]

[1] *Department of Transportation Engineering, Faculty of Engineering, Yalova University, 77200, Yalova, Turkey*

**Abstract**

In this paper, the applicability of relevance vector machine (RVM) has been explored to predict the ultimate axial load capacity of concrete-filled steel tube composite stub columns (CFSTCSCs) with circular sections under axial compression loadings. As an extension of support vector machine, RVM employs Bayesian inference to achieve parsimonious solutions for regression and classification. By using MATLAB software and 150 comprehensive experimental data presented in the previous studies, a model to predict the ultimate load of circular CFSTCSCs was developed by properly training the data. Utmost care has been taken in grouping the data for training and validation. About 80% dataset for training and 20% dataset for validation have been used, respectively. The results show that the predicted ultimate axial compression load capacity of CFSTCSC members is comparable with that of the corresponding experimental data and the percentage difference is about ∓11%.

**Keywords:** Concrete-filled steel tube composite stub columns (CFSTCSCs), Ultimate axial load capacity, Relevance vector machine (RVM), Nonlinear regression algorithm

**Özet**

Bu makalede, dairesel kesitli beton-dolgulu çelik tüplü kompozit kısa kolonların eksenel basınç yükleri altındaki nihai yük taşıma kapasitesini tahmin etmekte ilgililik vektör makinesinin (İVM) uygulanabilirliği incelenmiştir. Destek vektör makinesinin bir eklentisi olarak İVM, regresyon ve sınıflandırmada sağlam çözümler elde etmek için Bayesyen yaklaşımını kullanmaktadır. MATLAB yazılımı ve 150 adet daha önceki çalışmalarda sunulan kapsamlı deneysel veriler kullanılarak ve bu verilerin uygun şekilde düzenlenmesiyle, dairesel kesitli beton-dolgulu çelik tüplü kompozit kısa kolonların nihai yük taşıma kapasitesini tahmin etmek için bir model geliştirilmiştir. Verilerin düzenleme ve doğrulama için gruplandırılmasında azami özen gösterilmiştir. Sırasıyla, düzenleme için yaklaşık %80 veri seti ve doğrulama için %20 veri seti kullanılmıştır. Sonuçlar, beton-dolgulu çelik tüplü kompozit kolon elemanının tahmini nihai eksenel basınç yük taşıma kapasitesinin, ilgili deneysel verilerle kıyaslanabilir olduğunu ve aradaki yüzde farkının yaklaşık ∓%11 olduğunu göstermektedir.

**Anahtar kelimeler:** Beton-dolgulu çelik tüplü kompozit kısa kolonlar, Nihai eksenel yük taşıma kapasitesi, İlgililik vektör makinesi (İVM), Lineer olmayan regresyon algoritması

## 1 Introduction

Concrete-filled steel tube composite stub columns (CFSTCSCs) are being used in the civil infrastructure sector such as high-rise buildings, bridges, towers, etc., as they offer many structural advantages such as high strength, promising ductility, and large energy absorption capacities. The enhanced strength and ductility are due to the confinement of concrete. CFSTCSCs were used for various applications such as (i) retrofitting applications in earthquake-prone areas [1] (ii) bridge piers [2]. It was understood from the literature that the ultimate load of CFSTCSCs largely depends on material properties and steel ratio [3, 4] and several cross-sections of CFSTCSCs, namely, circular, square and rectangular, etc., were with various grades of concrete [5-10]. Design specifications used to predict the load capacity of composite stub columns, the ANSI/AISC 360–16 [11], and the Eurocode 4 (EC4) [12].

The axial compressive stiffness and ultimate capacity are the basic properties of CFSTCSCs. In the literature, there are different opinions and conclusions about the axial compressive stiffness of the stub columns, and one of the main reasons may be that researchers used different deformation measurement methods for the stub columns under axial compressive loading. However, there have been very few reports that compare these measurement methods for CFSTCSCs.

It is well known that analytical models are very much useful to predict the responses of the structural members. In the present scenario, machine learning techniques have attracted much importance to develop a model for the prediction of the future response. In any machine learning model, there are basically two major steps, namely, training, and testing. For training the data, mixed data with all variations should be required. One should have knowledge

* Sorumlu yazar / Corresponding author, e-posta / e-mail: cigdem.karatas@yalova.edu.tr (Ç. Avcı Karataş)
Geliş / Recieved: 28.06.2020 Kabul / Accepted:26.01.2021 Yayımlanma / Published: xx.xx.20xx
doi: 10.28948/ngmuh.759297

of the data preparation for training and testing. From the wide literature, it is noted that numerous statistical models or metamodels are available for developing the models to predict the required response. The models cover artificial neural networks, multivariate adaptive regression splines, Gaussian regression process, least squares support vector machine, relevance vector machine (RVM), and extreme learning machine, etc., to develop the models by training the mixed data [13-20].

After carefully study of the above models, it is observed that each model has its own advantages and limitations. RVM is a revised version of the support vector machine (SVM) and a machine learning methodology that uses Bayesian treatment to achieve parsimonious solutions for regression and classification [21, 22]. RVM is conceptualized under a complete probabilistic approach. In RVM, weights will be assigned to each dataset based on a defined algorithm and relate to hyperparameters. The significant feature of the RVM is that it uses very few kernel functions so that it will be computationally efficient. RVM concepts were used by many researchers in different domains for developing a model [23-29]. The applications of RVM concepts for the structural engineering domain are found to be scarce. When viewed from this aspect, this work will be a remarkable contribution to the existing knowledge base and engineers about the estimation of ultimate load capacity of CFSTCSCs based on RVM.

In the present study, RVM, one of the sophisticated statistical models is proposed to estimate the ultimate load capacity of CFSTCSCs with circular sections under axial loading by using the features of MATLAB. A dataset containing 150 experimental testing results available in the literature on CFSTCSC members under axial loading has been compiled for the present study.

## 2 Experimental dataset

Many experimental investigations were carried out by several researchers on the performance of circular CFSTCSCs under axial compression loading. The test configuration considered is the uniaxial compression test which is schematically depicted in Figure 1. A total of 150 data with 22 published literature sources has been collected from different sources. These experimental studies for stub/short CFSTCSCs have been compiled and the geometrical parameters, material strengths, and failure loads of various circular CFSTCSCs are tabulated in Table 1. It can be clearly sighted that the ultimate axial load capacity ($P_u$) is related to several variables such as (i) the outer diameter of steel tube, $D$ (ii) wall thickness of steel tube, $t$ (iii) unconfined concrete strength, $f_c$ (iv) Young's modulus of concrete, $E_c$ (v) yield strength of steel, $f_y$ (vi) Young's modulus of steel, $E_s$ (vii) length of circular CFSTCSC, $L$ (viii) confinement factor, $\xi$. Table 1 shows the geometrical parameters of CFSTCSCs sections, mechanical properties of steel and concrete, confinement factor, and failure load of a member under axial loadings. The compiled dataset has a wide range of column parameters such as normal to high yield strength steels ($f_y = 186\sim853\ MPa$), normal concrete to ultra-high-strength concrete ($f_c = 18\sim193\ MPa$), the outer diameter of circular sections ($D = 60\sim450\ mm$), the ratio of the outer diameter to the thickness ($D/t = 17\sim221$), and the ratio of the height to the outer diameter ($L/D = 1.8-4.9$), respectively. The aim of the developed model in the present research is to provide a unique study to the researcher to obtain the decreasing errors, complexity, and reducing convergence of scattering amplitudes of numerical results to the experimental ones that can be an alternative to experimental studies and to estimate the ultimate load capacity of circular CFSTCSCs. It can be obviously noted from Table 1 that $E_c$ varies between $17810\ MPa\sim66000\ MPa$ and for $E_s$, it varies in the range of $177000\ MPa$ and $213000\ MPa$. These variations have been considered while producing model processes to increase the possibility of obtaining a stronger model.

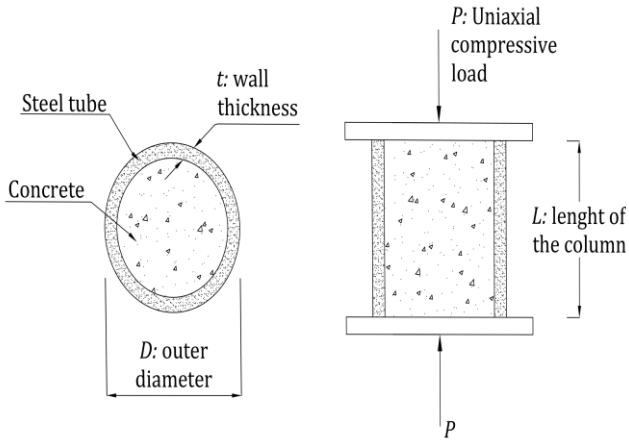


**Figure 1.** Geometrical configuration of CFSTCSC

## 3 Relevance vector machine (RVM)

RVM is a modified version of SVM, employs Bayesian concepts, and kernel function [21, 22]. RVM starts with the base of linear models, i.e., the function of $y(x)$ can be predicted at any point $x$ with a set of measurements of the function $t = (t_1, y, t_N)$ and with some training points $x = (x_1, y, x_N)$:

$$t_i = y(x_i) + \varepsilon_i \tag{1}$$

where $\varepsilon_i$ = the noise component of the measurement having mean 0 and variance $\sigma^2$. The unknown function $y(x)$ can be expressed as a linear combination of known basis function as

$$y(x) = \sum_{i=1}^{M} w_i \varphi_i(x) \tag{2}$$

where, $w_i = (w_1, y, w_M)$ = a vector consisting of the linear combination weights

$y(x)$ = output, a linearly weighted sum of $M$
$\varphi_i(x) = (\varphi_1(x), \varphi_2(x), \ldots\ldots, \varphi_M(M))^T$

For good predictions, most of the parameters are default set to zero [21, 22].

$$t = \Phi w + \varepsilon \tag{3}$$

where, $\Phi = NxM$ design matrix $\Phi_i(x)$ at all the training points

$\varepsilon_i = (\varepsilon_1, \dots, \varepsilon_N) =$ noise vector

RVM begins with a set of data input $\{x_n\}_n^N = 1$, and the associated vector $\{t_n\}_n^N = 1$. The prediction is of the form similar to SVM as given below:

$$y(x) = \sum_{i=1}^{N} w_i K(x, x_i) + w_0 \tag{4}$$

where, $w_i = w_1, w_2, \dots, w_N =$ weight vector
$K(x, x_i) =$ kernel function
$w_0 =$ bias function

Equation (5) shows the radial basis kernel function is employed in this work as follows:

$$K(x_i, x) = exp\left\{-\frac{(x_i - x)^T (x_i - x)}{2\sigma^2}\right\} \tag{5}$$

where $x_i$ and $x$ are the training and test patterns, $\sigma$ is the width of basis function, respectively. For a given input dataset, it is assumed as $\{x_n, t_n\}_n^N = 1$. It is assumed that $p(t|x)$ is Gaussian N (or Normal) $(t|y(x), \sigma^2)$. The mean of this distribution for a given $x$ can be modeled by $y(x)$ as mentioned in Equation (4). The likelihood of dataset can be written as

$$p(t|w, \sigma^2) = (2\pi\sigma^2)^{-N/2} exp\left\{-\frac{1}{2\sigma^2}\|t - \Phi w\|^2\right\} \tag{6}$$

where, $t_i = (t_1, \dots, t_N)^T$
$w_i = (w_0, \dots, w_N)$

$$\Phi^T = \begin{bmatrix} 1 & K(x_1, x_1) & K(x_1, x_2) & \cdots & K(x_1, x_n) \\ 1 & K(x_2, x_1) & K(x_2, x_2) & \cdots & K(x_2, x_n) \\ \vdots & \vdots & \vdots & \vdots & \vdots \\ 1 & K(x_n, x_1) & K(x_n, x_2) & \cdots & K(x_n, x_n) \end{bmatrix} \tag{7}$$

where $K(x_i, x_n)$ is the kernel function. The next higher-level parameters are useful to constrain an explicit zero-mean Gaussian prior probability distribution to the weights.

$$p(w|\alpha) = \prod_{i=0}^{N} N(w_i|0, \alpha_i^{-1}) \tag{8}$$

where $\alpha =$ a vector of $(N + 1)$ hyperparameters, useful for monitoring the weight deviations [25]. By applying Bayes' rule, the posterior unknowns can be computed as follows:

$$p(\alpha) = \prod_{i=0}^{N} Gamma(\alpha_i|a, b) \tag{9}$$

$$p(\beta) = \prod_{i=0}^{N} Gamma(\beta|c, d) \tag{10}$$

where, $\beta = \sigma^{-2}$. Hence, for $\alpha$ and $\sigma$, the distribution followed is gamma; for $w$, the normal distribution is followed and after the prior-distributions, Bayes' rule is followed.

$$p(w, \alpha, \sigma^2|t) = \frac{p(t|w, \alpha, \sigma^2) p(w, \alpha, \sigma^2)}{p(t)} \tag{11}$$

The predictive distribution for a new test point $(x*)$ corresponding to the target $(t*)$ is determined as

$$p(t*|t) = \int p(t*|w, \alpha, \sigma^2) p(w, \alpha, \sigma^2|t) dw\, d\alpha\, d\sigma^2 \tag{12}$$

By using the decomposition of posterior, the above equation can be solved as below in Equation (13):

$$p(w, \alpha, \sigma^2|t) = p(w|t, \alpha, \sigma^2) p(\alpha, \sigma^2|t) \tag{13}$$

The posterior distribution was analyzed by considering the appropriate weights due to the property of normalization integral is the convolution of Gaussians [22]. Accordingly, Equation (13) can be re-written as

$$p(w|t, \alpha, \sigma^2) = \frac{p(t|w, \sigma^2) p(w, \alpha)}{p(t|\alpha, \sigma^2)} \tag{14}$$

By using the Bayes' rule, Equation (14) can be modified as follows:

$$p(w|t, \alpha, \sigma^2) = (2\pi)^{-(N+1)/2} |\Sigma|^{-1/2} exp\left\{-\frac{1}{2}(w - \mu)^T \Sigma^{-1} (w - \mu)\right\} \tag{15}$$

The solution for the above equation is given below in Equation (16) and Equation (17):

$$\Sigma = (\sigma^{-2} \Phi^T \Phi + A)^{-1} \tag{16}$$

$$\mu = \sigma^{-2} \Sigma \Phi^T t \tag{17}$$

where, $\Sigma =$ covariance
$\mu =$ mean
$A = (\alpha_0, \alpha_1, \dots, \alpha_N)$

**Table 1.** Experimental data for ultimate axial load capacity of circular CFSTCSCs with the general details

| Source | Specimen | $D$ $(mm)$ | $t$ $(mm)$ | $f_c$ $(MPa)$ | $E_c$ $(MPa)$ | $f_y$ $(MPa)$ | $E_s$ $(MPa)$ | $L$ $(mm)$ | $\xi$ | $D/t$ | $L/D$ | $P_u$ $(kN)$ |
|---|---|---|---|---|---|---|---|---|---|---|---|---|
| [30, 31] | SPICIMEN8 | 120.8 | 4.06 | 34.40 | 27566 | 452 | 191536 | 241.3 | 1.962 | 30 | 2.0 | 1201 |
| | SPICIMEN9 | 120.8 | 4.09 | 29.58 | 25562 | 452 | 191536 | 241.4 | 2.300 | 30 | 2.0 | 1201 |
| | SPICIMEN10 | 120.8 | 4.09 | 25.92 | 23928 | 452 | 191536 | 241.4 | 2.625 | 30 | 2.0 | 1112 |
| | SPICIMEN13 | 152.6 | 3.18 | 20.89 | 21482 | 415 | 203395 | 304.8 | 1.766 | 48 | 2.0 | 1201 |
| | SPICIMEN14 | 152.6 | 3.15 | 23.10 | 22589 | 415 | 203395 | 304.8 | 1.581 | 48 | 2.0 | 1201 |
| | SPICIMEN4 | 101.7 | 3.07 | 31.16 | 26236 | 605 | 207050 | 203.3 | 2.575 | 33 | 2.0 | 1068 |
| | SPICIMEN3 | 101.7 | 3.07 | 34.13 | 27458 | 605 | 207050 | 203.3 | 2.351 | 33 | 2.0 | 1112 |
| | SPICIMEN3a | 169.3 | 2.62 | 36.54 | 28411 | 317 | 195811 | 305 | 0.563 | 65 | 1.8 | 1307 |
| [32] | 4HN | 150 | 4.3 | 28.71 | 25183 | 280 | 209720 | 450 | 1.222 | 35 | 3.0 | 1203 |
| | 4HN | 150 | 4.3 | 28.71 | 25183 | 280 | 209720 | 450 | 1.222 | 35 | 3.0 | 1225 |
| | 4HN | 150 | 4.3 | 28.71 | 25183 | 280 | 209720 | 450 | 1.222 | 35 | 3.0 | 1200 |
| | 3HN | 150 | 3.2 | 28.71 | 25183 | 287 | 190120 | 450 | 0.911 | 47 | 3.0 | 1040 |
| | 3HN | 150 | 3.2 | 28.71 | 25183 | 287 | 190120 | 450 | 0.911 | 47 | 3.0 | 998 |
| | 3HN | 150 | 3.2 | 28.71 | 25183 | 287 | 190120 | 450 | 0.911 | 47 | 3.0 | 980 |
| | 2HN | 150 | 2 | 28.71 | 25183 | 336 | 211680 | 450 | 0.65 | 75 | 3.0 | 882 |
| | 2HN | 150 | 2 | 28.71 | 25183 | 336 | 211680 | 450 | 0.65 | 75 | 3.0 | 882 |
| | 4MN | 150 | 4.3 | 21.95 | 22020 | 280 | 209720 | 450 | 1.599 | 35 | 3.0 | 1065 |
| | 4MN | 150 | 4.3 | 21.95 | 22020 | 280 | 209720 | 450 | 1.599 | 35 | 3.0 | 1087 |
| | 4MN | 150 | 4.3 | 21.95 | 22020 | 280 | 209720 | 450 | 1.599 | 35 | 3.0 | 1096 |
| | 3MN | 150 | 3.2 | 21.95 | 22020 | 287 | 190120 | 450 | 1.191 | 47 | 3.0 | 841 |
| | 3MN | 150 | 3.2 | 21.95 | 22020 | 287 | 190120 | 450 | 1.191 | 47 | 3.0 | 840 |
| | 3MN | 150 | 3.2 | 21.95 | 22020 | 287 | 190120 | 450 | 1.191 | 47 | 3.0 | 858 |
| | 2MN | 150 | 2 | 21.95 | 22020 | 336 | 211680 | 450 | 0.85 | 75 | 3.0 | 773 |
| | 2MN | 150 | 2 | 21.95 | 22020 | 336 | 211680 | 450 | 0.85 | 75 | 3.0 | 756 |
| | 4LN | 150 | 4.3 | 18.03 | 19957 | 280 | 209720 | 450 | 1.946 | 35 | 3.0 | 963 |
| | 3LN | 150 | 3.2 | 18.03 | 19957 | 287 | 190120 | 450 | 1.45 | 47 | 3.0 | 790 |
| | 3LN | 150 | 3.2 | 18.03 | 19957 | 287 | 190120 | 450 | 1.45 | 47 | 3.0 | 790 |
| | 3LN | 150 | 3.2 | 18.03 | 19957 | 287 | 190120 | 450 | 1.45 | 47 | 3.0 | 747 |
| | 2LN | 150 | 2 | 18.03 | 19957 | 336 | 211680 | 450 | 1.035 | 75 | 3.0 | 656 |
| | 2LN | 150 | 2 | 18.03 | 19957 | 336 | 211680 | 450 | 1.035 | 75 | 3.0 | 638 |
| | 2LN | 150 | 2 | 18.03 | 19957 | 336 | 211680 | 450 | 1.035 | 75 | 3.0 | 672 |
| [33] | L-20-1 | 178 | 9 | 22.15 | 22120 | 283 | 200000 | 360 | 3.036 | 20 | 2.0 | 2042 |
| | L-20-2 | 178 | 9 | 22.15 | 22120 | 283 | 200000 | 360 | 3.036 | 20 | 2.0 | 2102 |
| | H-20-1 | 178 | 9 | 45.37 | 31658 | 283 | 200000 | 360 | 1.482 | 20 | 2.0 | 2667 |
| | H-20-2 | 178 | 9 | 45.37 | 31658 | 283 | 200000 | 360 | 1.482 | 20 | 2.0 | 2677 |
| | L-32-1 | 179 | 5.5 | 22.15 | 22120 | 248 | 200000 | 360 | 1.514 | 33 | 2.0 | 1467 |
| | L-32-2 | 179 | 5.5 | 23.91 | 22982 | 248 | 200000 | 360 | 1.403 | 33 | 2.0 | 1530 |
| | H-32-1 | 179 | 5.5 | 43.61 | 31038 | 248 | 200000 | 360 | 0.769 | 33 | 2.0 | 2040 |
| | H-32-2 | 179 | 5.5 | 43.61 | 31038 | 248 | 200000 | 360 | 0.769 | 33 | 2.0 | 2030 |
| | L-58-1 | 174 | 3 | 23.91 | 22982 | 266 | 200000 | 360 | 0.809 | 58 | 2.1 | 1135 |
| | L-58-2 | 174 | 3 | 23.91 | 22982 | 266 | 200000 | 360 | 0.809 | 58 | 2.1 | 1135 |
| | H-58-1 | 174 | 3 | 45.67 | 31762 | 266 | 200000 | 360 | 0.423 | 58 | 2.1 | 1608 |
| | H-58-2 | 174 | 3 | 45.67 | 31762 | 266 | 200000 | 360 | 0.423 | 58 | 2.1 | 1677 |

**Table 1.** Experimental data for ultimate axial load capacity of circular CFSTCSCs with the general details (continued)

| Source | Specimen | $D$ $(mm)$ | $t$ $(mm)$ | $f_c$ $(MPa)$ | $E_c$ $(MPa)$ | $f_y$ $(MPa)$ | $E_s$ $(MPa)$ | $L$ $(mm)$ | $\xi$ | $D/t$ | $L/D$ | $P_u$ $(kN)$ |
|---|---|---|---|---|---|---|---|---|---|---|---|---|
| [34, 35] | R12CF1 | 190 | 1.15 | 110.3 | 32405 | 202 | 193200 | 662 | 0.045 | 165 | 3.5 | 2991 |
| | R12CF3 | 190 | 1.15 | 110.3 | 32405 | 202 | 193200 | 662 | 0.045 | 165 | 3.5 | 3137 |
| | S10CS50A | 190 | 0.86 | 41 | 17810 | 211 | 177000 | 659 | 0.094 | 221 | 3.5 | 1350 |
| | S12CS50A | 190 | 1.13 | 41 | 17810 | 186 | 178400 | 664.5 | 0.11 | 168 | 3.5 | 1377 |
| | S16CS50B | 190 | 1.52 | 48.3 | 21210 | 306 | 207400 | 664.5 | 0.208 | 125 | 3.5 | 1695 |
| | S20CS50A | 190 | 1.94 | 41 | 17810 | 256 | 204700 | 663.5 | 0.263 | 98 | 3.5 | 1678 |
| | S30CS50B | 165 | 2.82 | 48.3 | 21210 | 363 | 200600 | 580.5 | 0.541 | 59 | 3.5 | 1662 |
| | S10CS80B | 190 | 0.86 | 74.7 | 27576 | 211 | 177000 | 663.5 | 0.052 | 221 | 3.5 | 2451 |
| | S12CS80A | 190 | 1.13 | 80.2 | 28445 | 186 | 178400 | 662.5 | 0.056 | 168 | 3.5 | 2295 |
| | S16CS80A | 190 | 1.52 | 80.2 | 28445 | 306 | 207400 | 663.5 | 0.125 | 125 | 3.5 | 2602 |
| | S20CS80B | 190 | 1.94 | 74.7 | 27576 | 256 | 204700 | 663.5 | 0.144 | 98 | 3.5 | 2592 |
| | S30CS80A | 165 | 2.82 | 80.2 | 28445 | 363 | 200600 | 580.5 | 0.326 | 59 | 3.5 | 2295 |
| [36] | C1 | 140.8 | 3 | 28.18 | 25599 | 285 | 189475 | 602 | 0.92 | 47 | 4.3 | 790 |
| | C2 | 141.4 | 6.5 | 23.81 | 23528 | 313 | 206011 | 602 | 2.797 | 22 | 4.3 | 1332 |
| [37] | A1-1 | 125 | 1 | 106 | 48389 | 232 | 200000 | 438 | 0.072 | 125 | 3.5 | 1275 |
| | A1-2 | 125 | 1 | 106 | 48389 | 232 | 200000 | 438 | 0.072 | 125 | 3.5 | 1239 |
| | A2-1 | 127 | 2 | 106 | 48389 | 258 | 200000 | 445 | 0.161 | 64 | 3.5 | 1491 |
| | A2-2 | 127 | 2 | 106 | 48389 | 258 | 200000 | 445 | 0.161 | 64 | 3.5 | 1339 |
| | A3-1 | 133 | 3.5 | 106 | 48389 | 352 | 200000 | 465 | 0.379 | 38 | 3.5 | 1995 |
| | A3-2 | 133 | 3.5 | 106 | 48389 | 352 | 200000 | 465 | 0.379 | 38 | 3.5 | 1991 |
| | A4-1 | 133 | 4.7 | 106 | 48389 | 352 | 200000 | 465 | 0.524 | 28 | 3.5 | 2273 |
| | A4-2 | 133 | 4.7 | 106 | 48389 | 352 | 200000 | 465 | 0.524 | 28 | 3.5 | 2158 |
| | C-1 | 133 | 4.7 | 92 | 45081 | 352 | 200000 | 465 | 0.604 | 28 | 3.5 | 1854 |
| | C-2 | 133 | 4.7 | 92 | 45081 | 352 | 200000 | 465 | 0.604 | 28 | 3.5 | 1933 |
| | B-3 | 108 | 4.5 | 96 | 46050 | 358 | 200000 | 378 | 0.709 | 24 | 3.5 | 1518 |
| [38] | C10A-2A-3 | 101.8 | 3.03 | 23.2 | 22638 | 371 | 200000 | 305 | 2.088 | 34 | 3.0 | 628 |
| | C20A-2A | 216.4 | 6.61 | 24.3 | 23169 | 452 | 200000 | 650 | 2.499 | 33 | 3.0 | 3278 |
| | C30A-2A | 318.3 | 10.36 | 24.2 | 23121 | 335 | 200000 | 950 | 1.995 | 31 | 3.0 | 6319 |
| | C20A-4A | 216.4 | 6.61 | 46.8 | 32153 | 452 | 200000 | 650 | 1.298 | 33 | 3.0 | 4214 |
| | C10A-4A-1 | 101.9 | 3.03 | 51.3 | 33663 | 371 | 200000 | 305 | 0.943 | 34 | 3.0 | 877 |
| | C30A-4A | 318.5 | 10.36 | 52.2 | 33957 | 334 | 200000 | 950 | 0.921 | 31 | 3.0 | 8289 |
| [39] | CU-040 | 200 | 5 | 27.15 | 24490 | 266 | 200000 | 600 | 1.058 | 40 | 3.0 | 1951 |
| | CU-070 | 280 | 4 | 31.15 | 26232 | 273 | 200000 | 840 | 0.523 | 70 | 3.0 | 3025 |
| | CU-150 | 300 | 2 | 27.23 | 24526 | 342 | 200000 | 900 | 0.342 | 150 | 3.0 | 2608 |
| [3] | scv2-1 | 200 | 3 | 49.5 | 37420 | 304 | 206500 | 600 | 0.386 | 67 | 3.0 | 2383 |
| | scv2-2 | 200 | 3 | 49.5 | 37420 | 304 | 206500 | 600 | 0.386 | 67 | 3.0 | 2256 |
| [40] | C7 | 114.9 | 4.91 | 28.23 | 24972 | 365 | 200000 | 300.5 | 2.53 | 23 | 2.6 | 1020 |
| | C9 | 115 | 5.02 | 48.6 | 32765 | 365 | 200000 | 300.5 | 1.506 | 23 | 2.6 | 1378 |
| | C11 | 114.3 | 3.75 | 48.6 | 32765 | 343 | 200000 | 300 | 1.026 | 30 | 2.6 | 1033 |
| | C12 | 114.3 | 3.85 | 25.71 | 23831 | 343 | 200000 | 300 | 1.997 | 30 | 2.6 | 761 |
| | C4 | 114.6 | 3.99 | 83.6 | 42974 | 343 | 200000 | 300 | 0.637 | 29 | 2.6 | 1308 |

**Table 1.** Experimental data for ultimate axial load capacity of circular CFSTCSCs with the general details (continued)

| Source | Specimen | $D$ $(mm)$ | $t$ $(mm)$ | $f_c$ $(MPa)$ | $E_c$ $(MPa)$ | $f_y$ $(MPa)$ | $E_s$ $(MPa)$ | $L$ $(mm)$ | $\xi$ | $D/t$ | $L/D$ | $P_u$ $(kN)$ |
|---|---|---|---|---|---|---|---|---|---|---|---|---|
| [40] | C8 | 115 | 4.92 | 94.9 | 45786 | 365 | 200000 | 300 | 0.753 | 23 | 2.6 | 1787 |
| | C14 | 114.5 | 3.84 | 88.9 | 44315 | 343 | 200000 | 300 | 0.575 | 30 | 2.6 | 1359 |
| [41] | CC4-A-4-1 | 149 | 2.96 | 40.5 | 29911 | 308 | 200000 | 447 | 0.642 | 50 | 3.0 | 1064 |
| | CC8-A-8 | 108 | 6.47 | 77 | 41242 | 853 | 200000 | 324 | 3.221 | 17 | 3.0 | 2667 |
| | CC8-C-8 | 222 | 6.47 | 77 | 41242 | 843 | 200000 | 666 | 1.397 | 34 | 3.0 | 7304 |
| | CC8-D-8 | 337 | 6.47 | 85.1 | 43357 | 823 | 200000 | 1011 | 0.788 | 52 | 3.0 | 13776 |
| | CC4-D-4-1 | 450 | 2.96 | 41.1 | 30131 | 279 | 200000 | 1350 | 0.182 | 152 | 3.0 | 6870 |
| | CC4-D-4-2 | 450 | 3 | 41 | 30131 | 279 | 200000 | 1350 | 0.182 | 152 | 3.0 | 6985 |
| [4] | CA1-1 | 60 | 1.87 | 75.2 | 41540 | 282 | 201500 | 180 | 0.515 | 32 | 3.0 | 312 |
| | CA1-2 | 60 | 1.87 | 75.2 | 41540 | 282 | 201500 | 180 | 0.515 | 32 | 3.0 | 320 |
| | CA2-1 | 100 | 1.87 | 75.2 | 41540 | 282 | 201500 | 300 | 0.297 | 53 | 3.0 | 822 |
| | CA2-2 | 100 | 1.87 | 75.2 | 41540 | 282 | 201500 | 300 | 0.297 | 53 | 3.0 | 845 |
| | CA3-1 | 150 | 1.87 | 75.2 | 41540 | 282 | 201500 | 450 | 0.194 | 80 | 3.0 | 1701 |
| | CA3-2 | 150 | 1.87 | 75.2 | 41540 | 282 | 201500 | 450 | 0.194 | 80 | 3.0 | 1670 |
| | CA4-1 | 200 | 1.87 | 75.2 | 41540 | 282 | 201500 | 600 | 0.144 | 107 | 3.0 | 2783 |
| | CA4-2 | 200 | 1.87 | 75.2 | 41540 | 282 | 201500 | 600 | 0.144 | 107 | 3.0 | 2824 |
| | CA5-1 | 250 | 1.87 | 75.2 | 41540 | 282 | 201500 | 750 | 0.115 | 134 | 3.0 | 3950 |
| | CA5-2 | 250 | 1.87 | 75.2 | 41540 | 282 | 201500 | 750 | 0.115 | 134 | 3.0 | 4102 |
| | CB2-1 | 100 | 2 | 75.2 | 41540 | 404 | 207000 | 300 | 0.457 | 50 | 3.0 | 930 |
| | CB2-2 | 100 | 2 | 75.2 | 41540 | 404 | 207000 | 300 | 0.457 | 50 | 3.0 | 920 |
| | CB3-1 | 150 | 2 | 75.2 | 41540 | 404 | 207000 | 450 | 0.298 | 75 | 3.0 | 1870 |
| | CB3-2 | 150 | 2 | 75.2 | 41540 | 404 | 207000 | 450 | 0.298 | 75 | 3.0 | 1743 |
| | CB4-1 | 200 | 2 | 75.2 | 41540 | 404 | 207000 | 600 | 0.222 | 100 | 3.0 | 3020 |
| | CB4-2 | 200 | 2 | 75.2 | 41540 | 404 | 207000 | 600 | 0.222 | 100 | 3.0 | 3011 |
| | CB5-1 | 250 | 2 | 75.2 | 41540 | 404 | 207000 | 750 | 0.176 | 125 | 3.0 | 4442 |
| | CB5-2 | 250 | 2 | 75.2 | 41540 | 404 | 207000 | 750 | 0.176 | 125 | 3.0 | 4550 |
| | CC2-1 | 150 | 2 | 80 | 41540 | 404 | 207000 | 450 | 0.281 | 75 | 3.0 | 1980 |
| | CC2-2 | 150 | 2 | 80 | 41540 | 404 | 207000 | 450 | 0.281 | 75 | 3.0 | 1910 |
| | CC3-1 | 250 | 2 | 80 | 41540 | 404 | 207000 | 750 | 0.166 | 125 | 3.0 | 4720 |
| | CC3-2 | 250 | 2 | 80 | 41540 | 404 | 207000 | 750 | 0.166 | 125 | 3.0 | 4800 |
| [42] | D3M4C2 | 89.32 | 2.74 | 33 | 26999 | 360 | 200000 | 340 | 1.473 | 33 | 3.8 | 494 |
| | D3M4F13 | 89.32 | 2.74 | 31.48 | 26370 | 360 | 200000 | 340 | 1.544 | 33 | 3.8 | 495 |
| | D3M4F22 | 89.32 | 2.74 | 31.48 | 26370 | 360 | 200000 | 340 | 1.544 | 33 | 3.8 | 478 |
| | D3M4F33 | 89.32 | 2.74 | 28.19 | 24954 | 360 | 200000 | 340 | 1.724 | 33 | 3.8 | 529 |
| | D4M4C1 | 112.6 | 2.89 | 30.84 | 26101 | 360 | 200000 | 340 | 1.297 | 39 | 3.0 | 702 |
| | D4M4F13 | 112.6 | 2.89 | 31.48 | 26370 | 360 | 200000 | 340 | 1.271 | 39 | 3.0 | 757 |
| | D4M4F21 | 112.6 | 2.89 | 25.28 | 23631 | 360 | 200000 | 340 | 1.583 | 39 | 3.0 | 659 |
| | D4M4F32 | 112.6 | 2.89 | 26.2 | 24057 | 360 | 200000 | 340 | 1.527 | 39 | 3.0 | 638 |
| [43] | SZ3S4A1 | 165 | 2.72 | 48 | 32563 | 350 | 213000 | 510 | 0.506 | 61 | 3.1 | 1750 |
| | SZ3S6A1 | 165 | 2.73 | 67.2 | 38529 | 350 | 213000 | 510 | 0.363 | 60 | 3.1 | 2080 |

**Table 1.** Experimental data for ultimate axial load capacity of circular CFSTCSCs with the general details (continued)

| Source | Specimen | $D$ $(mm)$ | $t$ $(mm)$ | $f_c$ $(MPa)$ | $E_c$ $(MPa)$ | $f_y$ $(MPa)$ | $E_s$ $(MPa)$ | $L$ $(mm)$ | $\xi$ | $D/t$ | $L/D$ | $P_u$ $(kN)$ |
|---|---|---|---|---|---|---|---|---|---|---|---|---|
| [44] | C-30-3D | 114.3 | 3.35 | 32.7 | 26876 | 287 | 206000 | 342.9 | 1.128 | 34 | 3.0 | 669 |
| | C-60-3D | 114.3 | 3.35 | 58.7 | 36009 | 287 | 206000 | 342.9 | 0.629 | 34 | 3.0 | 946 |
| | C-80-3D | 114.3 | 3.35 | 88.8 | 44290 | 287 | 206000 | 342.9 | 0.416 | 34 | 3.0 | 1133 |
| | C-100-3D | 114.3 | 3.35 | 105.5 | 48275 | 287 | 206000 | 342.9 | 0.350 | 34 | 3.0 | 1455 |
| [45] | 049C36 30 | 360 | 6 | 31.5 | 26379 | 498 | 202000 | 1760 | 1.109 | 60 | 4.9 | 6888 |
| [46] | C3 | 114.3 | 3.6 | 173.5 | 63000 | 403 | 213000 | 250 | 0.323 | 32 | 2.2 | 2422 |
| | C4 | 114.3 | 3.6 | 173.5 | 63000 | 403 | 213000 | 250 | 0.323 | 32 | 2.2 | 2340 |
| | C5 | 114.3 | 3.6 | 184.2 | 63000 | 403 | 213000 | 250 | 0.304 | 32 | 2.2 | 2497 |
| | C6 | 114.3 | 3.6 | 184.2 | 63000 | 403 | 213000 | 250 | 0.304 | 32 | 2.2 | 2314 |
| | C7 | 114.3 | 6.3 | 173.5 | 63000 | 428 | 209000 | 250 | 0.649 | 18 | 2.2 | 2610 |
| | C8 | 114.3 | 6.3 | 173.5 | 63000 | 428 | 209000 | 250 | 0.649 | 18 | 2.2 | 2633 |
| | C9 | 219.1 | 5 | 51.6 | 28000 | 377 | 205000 | 600 | 0.684 | 44 | 2.7 | 3118 |
| | C10 | 219.1 | 5 | 185.1 | 66000 | 377 | 205000 | 600 | 0.199 | 44 | 2.7 | 7813 |
| | C11 | 219.1 | 5 | 193.3 | 66000 | 377 | 205000 | 600 | 0.191 | 44 | 2.7 | 8527 |
| | C12 | 219.1 | 10 | 51.6 | 28000 | 381 | 212000 | 600 | 1.489 | 22 | 2.7 | 4309 |
| | C13 | 219.1 | 10 | 185 | 66000 | 381 | 212000 | 600 | 0.435 | 22 | 2.7 | 9085 |
| | C14 | 219.1 | 10 | 193.3 | 66000 | 381 | 212000 | 600 | 0.416 | 22 | 2.7 | 9187 |
| | C15 | 219.1 | 6.3 | 163 | 66000 | 300 | 202000 | 600 | 0.231 | 35 | 2.7 | 6915 |
| | C16 | 219.1 | 6.3 | 175.4 | 59000 | 300 | 202000 | 600 | 0.215 | 35 | 2.7 | 7407 |
| | C17 | 219.1 | 6.3 | 148.8 | 52000 | 300 | 202000 | 600 | 0.254 | 35 | 2.7 | 6838 |
| | C18 | 219.1 | 6.3 | 174.5 | 52000 | 300 | 202000 | 600 | 0.216 | 35 | 2.7 | 7569 |
| [47, 48] | CF3-1 | 76.19 | 2.99 | 145 | 56595 | 278 | 200000 | 300 | 0.341 | 25 | 3.9 | 795 |
| | CF3.3-1 | 76.18 | 3.31 | 145 | 56595 | 305 | 200000 | 300 | 0.419 | 23 | 3.9 | 847 |
| | C4NG-1 | 114.2 | 4.02 | 115 | 50402 | 306 | 200000 | 400 | 0.418 | 28 | 3.5 | 1428 |
| | C6NG-1 | 114.3 | 5.98 | 115 | 50402 | 314 | 200000 | 400 | 0.675 | 19 | 3.5 | 1833 |
| [49] | c0 | 160 | 3.83 | 51 | 33900 | 409 | 200000 | 480 | 0.827 | 42 | 3.0 | 2023 |

Maximization of $p(\alpha, \alpha_{\epsilon_n}^2|\mathrm{y})\alpha\mathrm{p}(\mathrm{y}|\alpha, \alpha_{\epsilon_n}^2)p(\alpha)p(\alpha_{\epsilon_n}^2)$ concerning $\alpha$ and $\sigma^2$ provide a search for the hyperparameters posterior. For the case of uniform hyperpriors, maximization is to be performed for the terms of $p(y|\alpha, \alpha_{\epsilon_n}^2)$, as described below:

$$\begin{aligned}&\mathrm{p}(\mathrm{y}|\alpha, \alpha_{\epsilon_n}^2)\\ &= \int p(y|\mathrm{w}, \alpha_{\epsilon_n}^2)p(w|\alpha)\mathrm{dw} = (2\pi)^{-1/2}|\alpha_{\epsilon_n}^2\mathrm{I}\\ &+ \Phi A^{-1}\Phi^T|^{1/2}\mathrm{x}\exp\left\{-\frac{1}{2}y^T(|\alpha_{\epsilon_n}^2\mathrm{I}\right.\\ &\left.+ \Phi A^{-1}\Phi^T|)^{-1}y\right\}\end{aligned} \tag{18}$$

The predictions can be made based on the posterior distribution over the weights, conditioned on the maximized most probable values of $\alpha$, $\sigma_{\epsilon_n}^2$, $\alpha_{MP}$, and $\sigma_{MP}^2$, respectively.

$$\begin{aligned}&\mathrm{p}(\mathrm{y}*|\mathrm{y}, \alpha_{MP}, \sigma_{MP}^2)\\ &= \int p(y*|\mathrm{w}, \alpha_{MP}^2)p(w|\mathrm{y}, \alpha_{MP}, \sigma_{MP}^2)\mathrm{dw}\end{aligned} \tag{19}$$

Equation (19) can be evaluated as follows:

$$\mathrm{p}(\mathrm{y}*|\mathrm{y}, \alpha_{MP}, \sigma_{MP}^2) = \mathrm{N}(\mathrm{y}*|\mathrm{t}*, \sigma_*^2) \tag{20}$$

$$\mathrm{t}* = \mu^T\Phi(\mathrm{x}*) \tag{21}$$

$$\sigma_*^2 = \sigma_{MP}^2 + \Phi(\mathrm{x}*)^T\sum\Phi(x*) \tag{22}$$

The result of the optimization involved in RVM (i.e., max of $p(y|\alpha, \sigma_{\epsilon_n}^2)$), is that many of $\alpha$ tend to infinity such that "$w$" will have only a few nonzero weights that can be considered as relevant vectors [50].

## 4 RVM based analysis

In the present study, the main goal is to develop a model by using the concepts of RVM. To train the data and develop

a model, MATLAB software was used. The dependent parameters, such as $f_c$, $E_c$, $f_y$, $E_s$, $\xi$, $D/t$, and $L/D$ are considered as the input parameters for developing the RVM model. The output from the model is the ultimate load capacity of CFSTCSCs, $P_u$. There are a total of 150 datasets for training as well as validation. On closer examination of Table 1, the input vector has a significant variation in magnitude. Hence, a normalization of the data was done before inputting into the algorithm. Equation (23) has been used for the linear normalization of the data ranging between 0 and 1.

$$x_i^n = \frac{x_i^a - x_i^{min}}{x_i^{max} - x_i^{min}} \tag{23}$$

where $x_i^a$ and $x_i^n = i^{th}$ component of the input vector before and after normalization, $x_i^{max}$ and $x_i^{min}$ = the maximum and minimum values of all the components of the input vector before the normalization, respectively. About 80% of dataset was for training the data and about 20% of the dataset is used for testing and verification of the RVM model. The most important input parameter is the selection of kernel width. Further, the training and testing $R$ values are dependent on the number of relevance vectors (NRV) used in the model and their corresponding weights and variation in the kernel width. In the present study, the value of kernel width ($\sigma$) is assumed as 0.12. The efficiency of the model has been verified with the coefficient of correlation ($R$), which is given below:

$$R = \frac{\sum_{i=1}^{n}\left(E_{ai} - \overline{E}_a\right)\left(E_{pi} - \overline{E}_p\right)}{\sqrt{\sum_{i=1}^{n}\left(E_{ai} - \overline{E}_a\right)}\sqrt{\sum_{i=1}^{n}\left(E_{pi} - \overline{E}_p\right)}} \tag{24}$$

where $E_{ai}$ and $E_{pi}$ are the actual and predicted values, $\overline{E_a}$ and $\overline{E_p}$ are the mean of actual and predicted $E$ values corresponding to $n$ patterns, respectively. Figure 2 presents the schematic diagram of the RVM model. Table 2 presents the coefficient of correlation, the number of relevance vectors used in the development of the model. Table 3 shows the weights for the developed RVM model. By using Equation (18) and Equation (19) with $w_0$ as zero, the following equation has been deduced to predict $P_u$ values of CFSTCSC members under axial compression loadings. The values of weights, $w_i$, for all the training datasets are available in Table 3.

$$y = P_u = \sum_{i=1}^{105} w_i \, exp\left\{-\frac{\left(x_i - x\right)^T\left(x_i - x\right)}{0.034}\right\} \tag{25}$$

By using Equation (25), the normalized output vector has been converted back to original value as

$$x_i^a = x_i^n\left(x_i^{max} - x_i^{min}\right) + x_i^{min} \tag{26}$$

where, $x_i^n$ = normalized result obtained after the test for the $i^{th}$ component

$x_i^a$ =actual result obtained for $i^{th}$ component

$x_i^{max}$ and $x_i^{min}$ = maximum and minimum values of all the components of the corresponding input vector before the normalization

The developed model is applicable for the dataset in the range of yield strength of steels ($f_y = 186\sim853\ MPa$), concrete compressive strength ($f_c = 18\sim193\ MPa$), the outer diameter of circular sections ($D = 60\sim450\ mm$), the ratio of the outer diameter to the thickness ($D/t = 17\sim221$), and the ratio of the height to the outer diameter ($L/D = 1.8 - 4.9$). Table 4 presents the predicted ultimate axial load, $P_u^{RVM}$, and the corresponding experimental value, $P_u^E$. It can be very clearly seen that the predicted values by using the developed RVM model are comparable with each other. The maximum % difference between the predicted and the corresponding experimental value is about 11. The model can be used for the prediction of the ultimate load of CFSTCSC members under axial loading within the ranges of input data. The predicted values will be useful for the design of steel-concrete composite structures.

## 5 Conclusions

The concept of RVM has been employed for developing a model to predict the ultimate load of CFSTCSC members under axial loading. Large experimental data available in the literature on this concept has been collected. The data consists of large variations of geometry, mechanical properties, and ultimate loads. The influencing variables on the ultimate load have been identified after a close examination of the collected data. RVM is a machine learning methodology that uses Bayesian treatment to obtain parsimonious solutions for regression and classification. RVM is formulated based on the probabilistic concept and weights have been assigned iteratively and also related to a set of hyperparameters. RVM model was developed by using MATLAB software for training and prediction of the ultimate load capacity of CFSTCSCs. About 80% of the total datasets were used for training and about 20% of the remaining total datasets have been used for verification and validation of the developed model.

It was found that the predicted values are very much comparable with that of the corresponding experimental values. The predicted ultimate capacity is compared with that of the corresponding experimental value and the percentage difference between the predicted value and the corresponding experimental value is found to be less than 11%. The ratio of predicted and the corresponding experimental ultimate load $P_u^{RVM}/P_u^E$ was found to vary between 0.90 and 1.06, respectively.

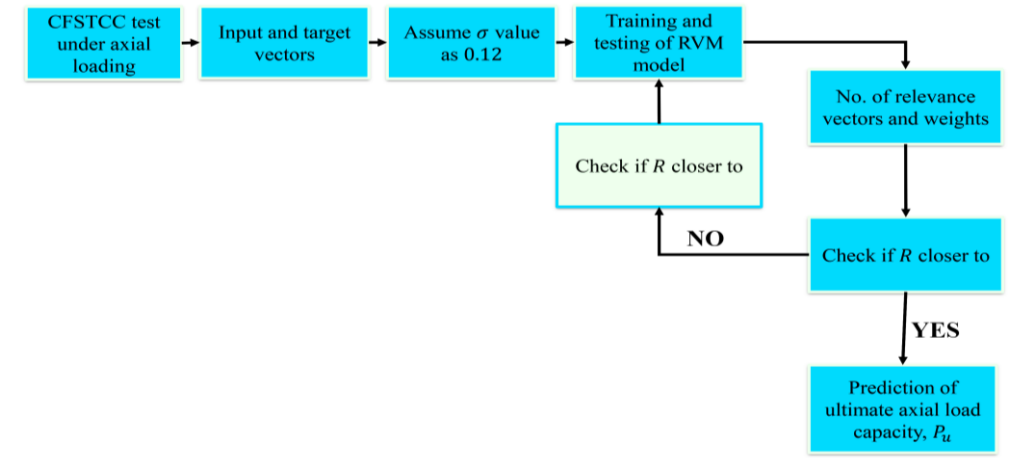


**Figure 2.** Schematic diagram for the proposed RVM model of CFSTCSC

**Table 2.** Performance of developed RVM models

| Parameters | Coefficient of correlation ($R$) | | Width | No. of RVs used out of total 105 dataset | No. of RVs (% of training dataset) |
|---|---|---|---|---|---|
| | Training | Testing | | | |
| $P_u$ | 0.996 | 0.991 | 0.12 | 85 | 80.5% |

**Table 3.** Weights ($w_i$) for RVM models

| $i = 1,2,\ldots,105$ | $w_i$ | $i = 1,2,\ldots,105$ | $w_i$ | $i = 1,2,\ldots,105$ | $w_i$ | $i = 1,2,\ldots,105$ | $w_i$ |
|---|---|---|---|---|---|---|---|
| 1 | 0.0 | 30 | 0.0 | 60 | 0.0 | 90 | 0.1 |
| 2 | 0.052 | 31 | 0.0 | 61 | 0.20 | 91 | 0.01 |
| 3 | 0 | 32 | 0.01 | 62 | 0.0 | 92 | 0.02 |
| 4 | 0 | 33 | 0.012 | 63 | 0.02 | 93 | 0.01 |
| 5 | 0.06 | 34 | 0.06 | 64 | 0.01 | 94 | 0.0 |
| 6 | 0.03 | 35 | 0.001 | 65 | 0.04 | 95 | 0.01 |
| 7 | 0.1 | 36 | 0.01 | 66 | 0.0 | 96 | 0.1 |
| 8 | 0.12 | 37 | 0.03 | 67 | 0.0 | 97 | 0.21 |
| 9 | 0.04 | 38 | 0.01 | 68 | 0.03 | 98 | 0.0 |
| 10 | 0.160 | 39 | 0.02 | 69 | 0.05 | 99 | 0.0 |
| 11 | 0.11 | 40 | 0.3 | 70 | 0.23 | 100 | 0.03 |
| 12 | 0.05 | 41 | 0.02 | 71 | 0.02 | 101 | 0.02 |
| 13 | 0.054 | 42 | 0.0 | 72 | 0.01 | 102 | 0.10 |
| 14 | 0.05 | 43 | 0.0 | 73 | 0.10 | 103 | 0.0 |
| 15 | 0.11 | 44 | 0.08 | 74 | 0.0 | 104 | 0.0 |
| 16 | 0.10 | 45 | 0.0 | 75 | 0.08 | 105 | 0.01 |
| 17 | 0.212 | 46 | 0.001 | 76 | 0.01 | | |
| 18 | 0.6 | 47 | 0.3 | 77 | 0.03 | | |
| 19 | 0.1 | 48 | 0.01 | 78 | 0.02 | | |
| 20 | 0.01 | 49 | 0.02 | 79 | 0.01 | | |
| 21 | 0.01 | 50 | 0.012 | 80 | 0.02 | | |
| 22 | 0.02 | 51 | 0.1 | 81 | 0.0 | | |
| 23 | 0.03 | 52 | 0.6 | 82 | 0.3 | | |
| 24 | 0.01 | 53 | 0.12 | 83 | 0.10 | | |
| 25 | 0.12 | 54 | 0.06 | 84 | 0.02 | | |
| 26 | 0.1 | 55 | 0.04 | 85 | 0.01 | | |
| 27 | 0.11 | 56 | 0.03 | 86 | 0.01 | | |
| 28 | 0.013 | 57 | 0.04 | 87 | 0.0 | | |
| 29 | 0.03 | 58 | 0.0131 | 88 | 0.01 | | |
| | | 59 | 0.013 | 89 | 0.03 | | |

**Table 4.** Comparison of experimental ultimate axial load values with predicted results obtained from RVM model

| $f_c$ $(MPa)$ | $f_y$ $(MPa)$ | $\xi$ | $D/t$ | $L/D$ | $P_u\ (kN)$ | | $P_u^{RVM}/P_u^E$ |
|---|---|---|---|---|---|---|---|
| | | | | | $P_u^E(kN)$ | $P_u^{RVM}(kN)$ | |
| 25.92 | 452 | 2.625 | 30 | 2.0 | 1112 | 1067 | 0.96 |
| 23.10 | 415 | 1.581 | 48 | 2.0 | 1201 | 1103 | 0.92 |
| 34.13 | 605 | 2.351 | 33 | 2.0 | 1112 | 1043 | 0.94 |
| 28.71 | 287 | 0.911 | 47 | 3.0 | 1040 | 1012 | 0.97 |
| 28.71 | 287 | 0.911 | 47 | 3.0 | 998 | 943 | 0.94 |
| 21.95 | 280 | 1.599 | 35 | 3.0 | 1087 | 1043 | 0.96 |
| 21.95 | 280 | 1.599 | 35 | 3.0 | 1096 | 1021 | 0.93 |
| 21.95 | 287 | 1.191 | 47 | 3.0 | 840 | 862 | 1.03 |
| 18.03 | 280 | 1.946 | 35 | 3.0 | 963 | 955 | 0.99 |
| 18.03 | 287 | 1.45 | 47 | 3.0 | 790 | 811 | 1.03 |
| 18.03 | 287 | 1.45 | 47 | 3.0 | 747 | 722 | 0.97 |
| 18.03 | 336 | 1.035 | 75 | 3.0 | 672 | 652 | 0.97 |
| 22.15 | 283 | 3.036 | 20 | 2.0 | 2102 | 2143 | 1.02 |
| 45.37 | 283 | 1.482 | 20 | 2.0 | 2667 | 2521 | 0.95 |
| 23.91 | 248 | 1.403 | 33 | 2.0 | 1530 | 1621 | 1.06 |
| 43.61 | 248 | 0.769 | 33 | 2.0 | 2030 | 2045 | 1.01 |
| 45.67 | 266 | 0.423 | 58 | 2.1 | 1608 | 1612 | 1.00 |
| 110.3 | 202 | 0.045 | 165 | 3.5 | 2991 | 2826 | 0.94 |
| 48.3 | 306 | 0.208 | 125 | 3.5 | 1695 | 1623 | 0.96 |
| 74.7 | 211 | 0.052 | 221 | 3.5 | 2451 | 2312 | 0.94 |
| 80.2 | 186 | 0.056 | 168 | 3.5 | 2295 | 2132 | 0.93 |
| 28.18 | 285 | 0.92 | 47 | 4.3 | 790 | 754 | 0.95 |
| 23.2 | 371 | 2.088 | 34 | 3.0 | 628 | 612 | 0.97 |
| 24.3 | 452 | 2.499 | 33 | 3.0 | 3278 | 3387 | 1.03 |
| 24.2 | 335 | 1.995 | 31 | 3.0 | 6319 | 6561 | 1.04 |
| 77 | 843 | 1.397 | 34 | 3.0 | 7304 | 7240 | 0.99 |
| 85.1 | 823 | 0.788 | 52 | 3.0 | 13776 | 14352 | 1.04 |
| 41.1 | 279 | 0.182 | 152 | 3.0 | 6870 | 6543 | 0.95 |
| 75.2 | 282 | 0.515 | 32 | 3.0 | 320 | 305 | 0.95 |
| 75.2 | 282 | 0.115 | 134 | 3.0 | 4102 | 3697 | 0.90 |
| 80 | 404 | 0.166 | 125 | 3.0 | 4800 | 4654 | 0.97 |

Hence the developed model will serve as a robust and reliable tool for the design of circular CFSTCSCs. The main focus of the present paper was to develop a model to predict the ultimate load capacity of CFSTCSCs based on RVM. Accordingly, the model was developed and the efficacy of the model was verified by the experimental data. The proposed model can be used in the modeling approach for the estimation of the ultimate load capacity of CFSTCSCs based on RVM.

**Acknowledgments**

Some or all raw/processed data required to reproduce these findings of this study will be made available from the corresponding author upon reasonable request. This research received no external funding. The author has no conflict of interest to declare the research described in this paper.

**Similarity rate (iThenticate):** 15%

**References**

[1] K. Sakino, Y. Sun, Steel jacketing for improvement of column strength and ductility. Proceedings of the 12th World Conference on Earthquake Engineering, New Zealand, February, 2000.

[2] O. I. Abdelkarim, A. Gheni, S. Anumolu, S. Wang, M. ElGawady, Hollow-core FRP-concrete-steel bridge columns under extreme loading. Report No. cmr15-008; Missouri Department of Transportation Research,

Development and Technology, Missouri University of Science and Technology, MO, USA, 2015.

[3] L. H. Han, G. H. Yao, Experimental behaviour of thin-walled hollow structural steel (HSS) columns filled with self-consolidating concrete (SCC). Thin-Walled Struct., 42(9), 1357–1377, 2004. https://doi.org/10.1016/j.tws.2004.03.016.

[4] L. H. Han, G. H. Yao, X. L. Zhao, Tests and calculations for hollow structural steel (HSS) stub columns filled with self-consolidating concrete (SCC). J. Constr. Steel Res., 61(9), 1241–1269, 2005. https://doi.org/10.1016/j.jcsr.2005.01.004.

[5] D. L. Liu, W. M. Gho, J Yuan, Ultimate capacity of high-strength rectangular concrete-filled steel hollow section stub columns. J. Constr. Steel Res., 59(12), 1499–1515, 2003. https://doi.org/10.1016/S0143-974X(03)00106-8.

[6] D. L. Liu, W. M. Gho, Axial load behaviour of high-strength rectangular concrete filled steel tubular stub columns. Thin-Walled Struct., 43(8), 1131–1142, 2005. https://doi.org/10.1016/j.tws.2005.03.007.

[7] D. M. Lue, J. L. Liu, T. Yen, Experimental study on rectangular CFST columns with high-strength concrete. J. Constr. Steel Res., 63(1), 37–44, 2007. https://doi.org10.1016/j.jcsr.2006.03.007.

[8] Q. Yu, Z. Tao, Y. X. Wu, Experimental behaviour of high performance concrete filled steel tubular columns. Thin-Walled Struct., 46(4), 362–370, 2008. https://doi.org/10.1016/j.tws.2007.10.001.

[9] B. Uy, Strength of short concrete filled high strength steel box columns. J. Constr. Steel Res., 57(2), 113–134, 2001. https://doi.org/10.1016/S0143974X(00)00014-6.

[10] F. Aslani, B. Uy, Z. Tao, F. Mashiri, Behaviour and design composite columns incorporating compact high-strength steel plates. J. Constr. Steel Res., 107, 94–110, 2015. https://doi.org/10.1016/j.jcsr.2015.01.005.

[11] ANSI/AISC-360-10, Specification for Structural Steel Buildings. Illinois 60601-1802, American Institute of Steel Construction, Chicago, 2010. https://www.aisc.org/Specification-for-Structural-Steel-Buildings-ANSIAISC-360-16-1.

[12] Eurocode 4: EN 1994-1-1 (2004) (English): Design of composite steel and concrete structures – Part 1-1: General rules and rules for buildings [Authority: The European Union per Regulation 305/2011, Directive 98/34/EC, Directive 2004/18/EC]. https://eurocodes.jrc.ec.europa.eu/showpage.php?id=134.

[13] P. Yuvaraj, A. R. Murthy, N. R. Iyer, P. Samui, S. K. Sekar, Multivariate adaptive regression splines model to predict fracture characteristics of high strength and ultra high strength concrete beams. Comput. Mater. Contin., 36(1), 73–97, 2013. https://doi.org/10.3970/cmc.2013.036.073.

[14] P. Yuvaraj, A. R. Murthy, N. R. Iyer, P. Samui, S. K. Sekar, Prediction of fracture characteristics of high strength and ultra high strength concrete beams based on relevance vector machine. Int. J. Damage Mech., 23(7), 979–1004, 2014. https://doi.org/10.1177/1056789514520796.

[15] S. Dutta, A. R. Murthy, D. Kim, P. Samui, Prediction of compressive strength of self-compacting concrete using intelligent computational modelling. Comput. Mater. Contin., 53(2), 157-174, 2017. https://doi.org/10.3970/cmc.2017.053.167.

[16] J. Kaur, K. Kaur, A fuzzy approach for an IoT-based automated employee performance appraisal. Comput. Mater. Contin., 53(1), 23–36, 2017. https://doi.org/10.3970/cmc.2017.053.024.

[17] A. R. Murthy, S. Vishnuvardhan, M. Saravanan, P. Gandhi, Relevance vector based approach for the prediction of stress intensity factor for the pipe with circumferential crack under cyclic loading. Struct. Eng. Mech., 72(1), 31–41, 2019. https://doi.org/10.12989/sem.2019.72.1.031.

[18] P. K. Prasanna, A. R. Murthy, K. Srinivas, Prediction of compressive strength of GGBS based concrete using RVM. Struct. Eng. Mech., 68(6), 691–700, 2018. https://doi.org/10.12989/sem.2018.68.6.691.

[19] C. Avci-Karatas, Prediction of ultimate load capacity of concrete-filled steel tube columns using multivariate adaptive regression splines (MARS). Steel Compos. Struct., 33(4), 583–594, 2019. https://doi.org/10.12989/scs.2019.33.4.583.

[20] A. Gholampour, I. Mansouri, O. Kisi, T. Ozbakkaloglu, Evaluation of mechanical properties of concretes containing coarse recycled concrete aggregates using multivariate adaptive regression splines (MARS), M5 model tree (M5Tree), and least squares support vector regression (LSSVR) models. Neural Comput. Appl., 32, 295–308, 2020. https://doi.org/10.1007/s00521-018-3630-y.

[21] M. E. Tipping, Sparse Bayesian learning and the relevance vector machine. J. Mach. Learn. Res., 1, 211–244, 2001.

[22] M. E. Tipping, The relevance vector machine. In S. A. Solla, T. K. Leen, and K.-R. Muller, editors, Advances in Neural Information Processing Systems, 12, 652–658, 2000.

[23] L. Wei, Y. Yang, R. M. Nishikawa, M. N. Wernick, A. Edwards, Relevance vector machine for automatic detection of clustered micro-calcifications. IEEE Transactions on Medical Imaging, 24(10), 1278–1285, 2005. https://doi.org/10.1109/TMI.2005.855435.

[24] S. K. Das, P. Samui, Prediction of liquefaction potential based on CPT data: A relevance vector machine approach. Proceedings of the 12th International Conference of International Association for Computer Methods and Advances in Geomechanics (IACMAG), October, 2008, Goa, India, 2008.

[25] W. Caesarendra, A. Widodo, B. S. Yang, Application of relevance vector machine and logistic regression for machine degradation assessment. J. Mech. Syst. Signal Process., 24, 1161–1171, 2009. https://doi.org/10.1016/j.ymssp.2009.10.011.

[26] X. Wang, M. Ye, C. J. Duanmu, Classification of data from electronic nose using relevance vector machines.

Sens. Actuators B Chem., 140(1), 143–148, 2009. https://doi.org/10.1016/j.snb.2009.04.030.
[27] K. Liu, Z. Xu, Traffic flow prediction of highway based on wavelet relevance vector machine. J. Inf. Comput. Sci., 8(9), 1641–1647, 2011.
[28] M. H. Stanikzai, S. Elias, R. Rupakhety, Seismic response mitigation of base-isolated buildings. Appl. Sci., 10(4), 1230, 2020. https://doi.org/10.3390/app10041230.
[29] H. Dehghani, I. Mansouri, A. Farzampour, J. W. Hu, Improved homotopy perturbation method for geometrically nonlinear analysis of space trusses, Appl. Sci., 10(8), 2987, 2020. https://doi.org/10.3390/app10082987.
[30] N. J. Gardener, R. Jacobson, Structural behavior of concrete filled steel tubes. J. Am. Concr. Inst., 64(7), 404–413, 1967.
[31] N. J. Gardener, Use of spiral welded steel tubes in pipe columns. J. Am. Concr. Inst., 65(11), 937–942, 1968.
[32] M. Tomii, K. Yoshimura, Y. Morishita, Experimental studies on concrete filled steel tubular stub columns under concentric loading. Proceedings of the International Colloquium on Stability of Structures under Static and Dynamic Loads, Washington, USA, May, 718–741, 1977.
[33] K. Sakino, H. Hayashi, Behavior of concrete filled steel tubular stub columns under concentric loading. Proceedings of the 3rd International Conference on Steel Concrete Composite Structures, Fukuoka, Japan, September, 25–30, 1991.
[34] M. D. O'Shea, R. Q. Bridge, Tests of thin-walled concrete-filled steel tubes. Proceedings of the 12th International Specialty Conference on Cold-Formed Steel Structures, St. Louis, USA, October, 399–419, 1994. https://scholarsmine.mst.edu/isccss/12iccfss/12iccfss-session7/3.
[35] M. D. O'Shea, R. Q. Bridge, Tests on circular thin-walled steel tubes filled with medium and high strength concrete. Australian Civil Engineering Transaction, 40, 15–27, 1998.
[36] S. P. Schneider, Axially loaded concrete-filled steel tubes. J. Struct. Eng., 124(10), 1125–1138, 1998. https://doi.org/10.1061/(ASCE)07339445(1998)124:10(1125).
[37] K. F. Tan, X. C. Pu, S. H. Cai, Study on mechanical properties of extra-high strength concrete encased in steel tubes, J. Build. Struct., 20(1), 10–15, 1999. http://manu25.magtech.com.cn/Jwk3_jzjgxb.
[38] T. Yamamoto, J. Kawaguchi, S. Morino, Experimental study of scale effects on the compressive behavior of short concrete-filled steel tube columns, Proceedings of the United Engineering Foundation Conference on Composite Construction in Steel and Concrete IV (AICE), Banff, Canada, June, 879–891, 2000. https://doi.org/10.1061/40616(281)76.
[39] C. S. Huang, Y. K. Yeh, G. Y. Liu, H. T. Hu, K. C. Tsai, Y.T. Weng, S. H. Wang, M. H. Wu, Axial load behavior of stiffened concrete-filled steel columns. J. Struct. Eng., 128(9), 1222–1230, 2002. https://doi.org/10.1061/(ASCE)07339445(2002)128:9(1222).
[40] G. Giakoumelis, D. Lam, Axial capacity of circular concrete-filled tube columns, J. Constr. Steel Res., 60(7), 1049–1068, 2004. https://doi.org/10.1016/j.jcsr.2003.10.001.
[41] K. Sakino, H., Nakahara, S. Morino, I. Nishiyama, Behavior of centrally loaded concrete-filled steel-tube short columns, J. Struct. Eng., 130(2), 180–188, 2004. https://doi.org/10.1061/(ASCE)07339445(2004)130:2(180).
[42] P. K. Gupta, S. M. Sarda, M. S. Kumar, Experimental and computational study of concrete filled steel tubular columns under axial loads. J. Constr. Steel Res., 63(2), 182–193, 2007. https://doi.org/10.1016/j.jcsr.2006.04.004.
[43] Z. W. Yu, F. X. Ding, C. S. Cai, Experimental behavior of circular concrete filled steel tube stub columns. J. Constr. Steel Res., 63, 165–174, 2007. https://doi.org/10.1016/j.jcsr.2006.03.009.
[44] W. L.A. de Oliveira, S. de Nardin, A. L. H. de Cresce El Debs, M. K. El Debs, Influence of concrete strength and length/diameter on the axial capacity of CFT columns. J. Constr. Steel Res., 65(12), 2103–2110, 2009. https://doi.org/10.1016/j.jcsr.2009.07.004.
[45] S. H., Lee, B. Uy, S. H. Kim, Y. H. Choi, S. M. Choi, Behavior of high-strength circular concrete-filled steel tubular (CFST) column under eccentric loading. J. Constr. Steel Res., 67, 1–13, 2011. https://doi.org/10.1016/j.jcsr.2010.07.003.
[46] M. X., Xiong, D. X. Xiong, J. Y. R. Liew, Axial performance of short concrete filled steel tubes with high- and ultra-high- strength materials. Eng. Struct., 136, 494–510, 2017. https://doi.org/10.1016/j.engstruct.2017.01.037.
[47] S. Guler, A. Copur, M. Aydogan, Axial capacity and ductility of circular UHPC-filled steel tube columns. Mag. Concrete Res., 65(15), 898–905, 2013. https://doi.org/10.1680/macr.12.00211.
[48] S. Guler, A. Copur, M. Aydogan, A comparative study on square and circular high strength concrete-filled steel tube columns. Adv. Steel Constr., 10(2), 234–247, 2014. https://doi.org/10.18057/IJASC.2014.10.2.7.
[49] L. H., Han, C. C. Hou, Q. L. Wang, Behavior of circular CFST stub columns under sustained load and chloride corrosion. J. Constr. Steel Res., 103, 23–36, 2014. https://doi.org/10.1016/j.jcsr.2014.07.021.
[50] S. Ghosh, P. P. Mujumdar, Statistical downscaling of GCM simulations to streamflow using relevance vector machine. Adv. Water Resour., 31(1), 132–146, 2008. https://doi.org/10.1016/j.advwatres.2007.07.005.